Boson-Gutzwiller quantum liquids on a lattice

Daniel Pérez-Cruz [1] and Manuel Valiente [2]
[1]Departamento de Física and IUdEA, Universidad de La Laguna, 38206 La Laguna, Tenerife, Spain
[2]Departamento de Física, CIOyN, Universidad de Murcia, 30071 Murcia, Spain

(Received 25 February 2025; accepted 11 June 2025; published 26 June 2025)

We consider one-dimensional, interacting spinless bosons on a tight-binding lattice described by the Bose-Hubbard model. Besides attractive onsite two-body interactions, we include a three-body repulsive term such that the competition between these two forces allows the formation of self-bound liquid states. We investigate the properties of this system using the Gutzwiller approximation, showing that, indeed, this mean-field approach also supports liquid states. We find that for densities lower than the equilibrium density, the Gutzwiller method and other mean-field approaches—such as the Gross-Pitaevskii theory—feature a sharp transition to the vacuum state. This, however, is avoided by considering local minima of the functional in the standard manner. We also study the excitation spectrum, and calculate the speed of sound, in full agreement with the usual expression obtained from the thermodynamic equation of state. We study their corresponding quantum droplets variationally and find that the results behave in accordance with the one-dimensional liquid-drop model.

DOI: 10.1103/lvqx-g5l2

I. INTRODUCTION

A quantum liquid, strictly speaking, is defined as a spatially homogeneous system of interacting particles at temperatures sufficiently low that the effects of quantum statistics are important [1]. These systems provide ideal playgrounds for exploring many-body physics, quantum phase transitions, and emergent phenomena that arise from strong interactions. The study of quantum liquids, meaning those that form self-bound states—droplets—in vacuum, and feature equilibrium properties typical of a liquid in the thermodynamic limit, has gained significant attention due to advances in ultracold atom experiments, which allow for precise control over interactions, confinement, and dimensionality [2–7].

In particular, we are interested in the possibility of confining these systems to one-dimensional geometries. This enhances interaction effects, making them highly controllable platforms for investigating strongly correlated matter. As a result, new avenues have been opened for studying quantum droplets and novel liquidlike phases of matter [8–11].

Here we include two- and three-body interactions between bosons to stabilize a zero-temperature liquid on a lattice [11]. Three-body processes are always present in many-body systems. Still, their origin may be either a true three-body interparticle potential or an emergent residual interaction from the off-shell structure of the two-body potential [12–15]. In one-dimensional geometries, the competition between mean-field repulsion and beyond-mean-field attraction results in the formation of quantum liquid droplets, marking a fundamental advancement in our understanding of low-dimensional quantum fluids.

Even though mean-field methods perform better in higher dimensions, their application to one-dimensional systems still gives successful results. The bosonic Gutzwiller ansatz provides valuable insights into strongly correlated bosonic systems and bridges more sophisticated numerical techniques and experimental observations [16–18]. Its simplicity and adaptability make it a valuable tool in the study of ultracold atoms in optical lattices. These simpler approaches yield qualitatively correct phase diagrams and excitation spectra, particularly away from critical points. A comparison is made with available density-matrix renormalization group (DMRG) data in one dimension, from Ref. [11]; this serves to quantify both the strengths and limitations of the mean-field approach in this context.

In this work, we make use of the Gutzwiller ansatz to variationally study both ground-state properties and low-energy excitations of a Bose-Hubbard model [19,20] with two- and three-body contact interactions, and show that it does support a zero-temperature liquid state. We also study the formation of quantum droplets in finite systems and analyze their properties as a function of the number of particles.

II. MODEL AND METHOD

We consider ultracold bosons on a tight-binding lattice interacting via contact two- and three-body interactions [21]. This system is known to support a quantum liquid (droplet) ground state in the thermodynamic limit (vacuum), for combined attractive two-body and repulsive three-body potentials in one dimension [11]. The corresponding Hamiltonian is given by

$$H = -J\sum_j [b_j^\dagger b_{j+1} + b_{j+1}^\dagger b_j - 2n_j] + H_{\rm I}, \qquad (1)$$

where J (>0) is the tunneling rate, b_j ($b_j^\dagger$) is the bosonic annihilation (creation) operator at site j, $n_j = b_j^\dagger b_j$ is the corresponding number operator, and we have set the lattice spacing $d = 1$. The interaction is given by

$$H_{\rm I} = \frac{U}{2}\sum_j n_j(n_j-1)\left[1+\frac{W}{3U}(n_j-2)\right], \tag{2}$$

where U (<0) and W (>0) are, respectively, the two- and three-body interaction strengths.

We shall use the Boson-Gutzwiller mean-field method at zero temperature to study the thermodynamic equation of state and low-energy excitations, as well as the droplets of the system in vacuum. The method is variational, and the underlying wave function—the Gutzwiller ansatz—takes the following form [22–25]:

$$|\Psi\rangle = \bigotimes_j |\phi_j\rangle, \quad |\phi_j\rangle = \sum_{n=0}^{\infty} a_n(j)|n_j\rangle, \tag{3}$$

where $|n_j\rangle$ is the Fock state with n particles at site j, and $a_n(j)$ are the expansion coefficients. Since the Gutzwiller wave function, Eq. (3), does not have a fixed particle number, we work in the grand-canonical ensemble, that is, we use the grand potential Ω in place of the Hamiltonian H, with $\Omega = H - \mu N$, where $N = \sum_j n_j$ is the total number operator, and μ is the chemical potential.

The simplicity of the Gutzwiller ansatz allows us to study a wide range of system properties in a simple and clear manner. This approach is equivalent (at zero temperature) to the following decoupling approximation

$$b_i^\dagger b_j \approx \langle b_i^\dagger\rangle b_j + \langle b_j\rangle b_i^\dagger - \langle b_j\rangle\langle b_i^\dagger\rangle, \tag{4}$$

as was shown in Ref. [26]. We note that the bosonic Gutzwiller approximation can also be extended to account for quantum fluctuations [27,28] around the mean-field solution.

The relevant local quantity that characterizes the behavior of the system is the superfluid order parameter ψ_j at site j, defined as

$$\psi_j = \langle b_j\rangle = \sum_{n=0}^{\infty} a_n^*(j)a_{n-1}(j)\sqrt{n}. \tag{5}$$

The superfluid density at site j is given by $|\psi_j|^2$, and is bounded from above by the total number of particles at site j, is given by

$$\langle n_j\rangle = \sum_{n=0}^{\infty} n|a_n(j)|^2. \tag{6}$$

III. HOMOGENEOUS SYSTEM AND EQUATION OF STATE

We first consider a homogeneous system with uniform density, that is, in the thermodynamic limit. This brings a major simplification of the problem since all local wave functions $|\phi_j\rangle$ in Eq. (3) become identical (site independent). Therefore, we define, for all j,

$$|\phi_j\rangle \equiv |\phi\rangle = \sum_n a_n|n\rangle. \tag{7}$$

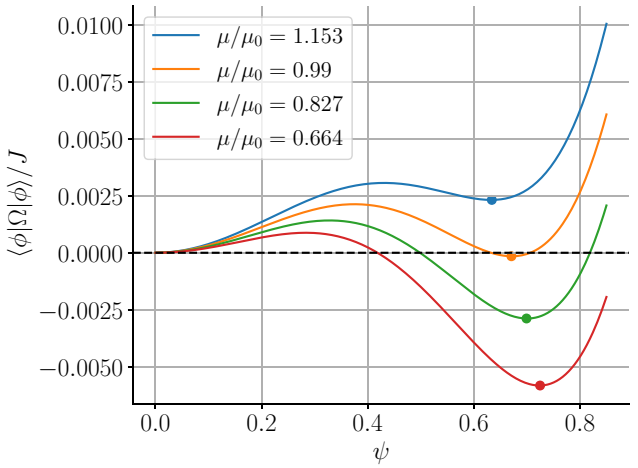

FIG. 1. Energy landscape of the grand-canonical function in terms of the order parameter ψ. The dots represent the local minimum that gives us the nonzero solution for the system's ground state. It is clear that, as the equilibrium density is crossed, the vacuum becomes, energetically, the most favorable solution. The parameters of the Hamiltonian Eq. (9) are $U/J = -0.33$, $W/J = 1.39$.

The problem can be more conveniently formulated by simplifying the Hamiltonian through the decoupling approximation, Eq. (4), which is especially simple in the homogeneous case.

Upon decoupling the Hamiltonian, the minimization of the grand potential Ω reduces to a single-site problem, since

$$\langle\Psi|\Omega|\Psi\rangle \equiv \sum_j \langle\phi|\Omega_j|\phi\rangle, \tag{8}$$

where the single-site grand-canonical Hamiltonian Ω_j has the form

$$\Omega_j = -2J[b_j^\dagger\psi + \psi^* b_j] + (2J-\mu)n_j + 2J|\psi|^2 + \frac{U}{2}n_j(n_j-1)\left[1+\frac{W}{3U}(n_j-2)\right]. \tag{9}$$

To see whether a zero-temperature quantum liquid exists, within the Gutzwiller approximation, we minimize the single-site grand-canonical Hamiltonian with fixed values of μ. In all cases, we find that the global minimum is attained with nonzero densities ρ when these are higher than the equilibrium density ρ_0. If we call the spinodal density ρ_*, then for $\rho_* < \rho < \rho_0$, the state that analytically continues the zero-temperature equation of state gives no longer the global minimum, but becomes a local one (see Fig. 1). This is not a feature particular to the Gutzwiller approximation, but common to other mean-field theories. This is thoroughly discussed in Appendix A, where we demonstrate the occurrence of a first-order transition to the vacuum state at the equilibrium density in the context of the Gross-Pitaevskii equation.

Proceeding, in our case, by accepting the local minimum with nonzero density as the solution, we show in Fig. 2 the equation of state (EoS) for two particular values U and W of the two- and three-body interaction strengths. There, we see the formation of a liquid state, with an equilibrium density ρ_0 at the minimum of the energy per particle, and a spinodal point ρ_*, for which $\partial\mu/\partial\rho|_{\rho=\rho_*} = 0$. The spinodal point marks

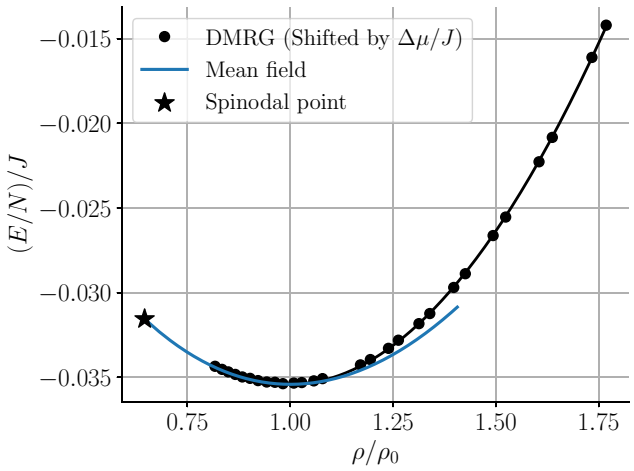

FIG. 2. Equation of state of a quantum liquid obtained by means of the Gutzwiller ansatz and comparison with DMRG data from Ref. [11]. We have rescaled the x axis by its corresponding equilibrium density ($\rho_0^{\mathrm{DMRG}} d = 0.576$ and $\rho_0^{\mathrm{MF}} d = 0.450$) and also shifted the DMRG data by $\Delta\mu/J = (e_0^{\mathrm{MF}} - e_0^{\mathrm{DMRG}})/J = 0.00489$, further details are given in the text. The parameters of Hamiltonian Eq. (9) are $U/J = -0.33$, $W/J = 1.39$.

the density below which the system is unstable against the formation of droplets. Note that, as opposed to the Gross-Pitaevskii approach (see, e.g., Ref. [29]), with the Gutzwiller ansatz there is no solution beyond the spinodal point, i.e., no solution has density $\rho < \rho_*$. We compare our results with exact DMRG calculations in one dimension [11]. To enable a meaningful comparison between the two approaches, we normalize the densities to their respective equilibrium values and shift the energy scales to align the minima. The equilibrium chemical potential from the Gutzwiller approximation is off by only about 1.5% from the exact DMRG calculation. Despite these necessary adjustments, the central conclusion of our study remains: using a significantly simpler analytical approach, we are able to capture the essential qualitative behavior of an otherwise challenging problem, showing that, indeed, a quantum liquid is formed in this system.

From the equation of state, we calculate the speed of sound c using the familiar relation

$$mc^2 = \frac{\partial \mu}{\partial N}, \tag{10}$$

where the mass is to be identified with the tight-binding expression $J = \hbar^2/2md^2$. In the next section, we calculate the speed of sound directly from the low-energy excitation spectrum and compare the results.

IV. INHOMOGENEOUS SYSTEM AND LOW-ENERGY EXCITATIONS

In general, the Gutzwiller ansatz allows us to explore the dynamics of nonuniform systems. With the parametrization of the ground-state ansatz in Eq. (3), we now find the set of parameters $\{a_n(j)\}$ that minimizes the grand potential $\Omega = H - \mu N$, with the Hamiltonian H of Eq. (1). To do so, we have two equivalent options: (i) we apply the decoupling approximation of Eq. (4) to the grand potential; or (ii) we use directly the Gutzwiller ansatz, Eq. (3), and minimize the Lagrangian $\mathcal{L} = H - \mu N - i\partial_t$ (we set $\hbar \equiv 1$) to allow for time-dependent dynamics.

We proceed with approach (ii), with time-dependent amplitudes $a_n(j;t)$, which gives the following set of time-dependent Gutzwiller equations ($\hbar \equiv 1$) [30,31]:

$$i\frac{da_n(j;t)}{dt} = \sum_{m=0}^{\infty} \Omega_j(n,m) a_m(j;t), \tag{11}$$

where the site-dependent matrix elements $\Omega_j(n,m)$ have the form

$$\begin{aligned}\Omega_j(n,m) = &\left[\frac{U}{2}(n-1) + \frac{W}{6}(n-1)(n-2)\right.\\ &\left. + (2J-\mu)\right] n\delta_{n,m} + J(\psi_{j+1}^* + \psi_{j-1}^*)\psi_j \delta_{n,m}\\ &- J\sqrt{m}(\psi_{j+1}^* + \psi_{j-1}^*)\delta_{m,n+1}\\ &- J\sqrt{n}(\psi_{j+1} + \psi_{j-1})\delta_{n,m+1}.\end{aligned} \tag{12}$$

A. Low-energy excitations

To extract low-energy excitations, we consider plane-wave perturbations moving on top of the ground state as

$$a_n(j;t) = a_n^{(0)} + a_n^{(1)}(j;t) + \ldots, \tag{13}$$

where $a_n^{(0)}$ is the n-particle amplitude of the ground=state wave function, Eq. (7), in the homogeneous, thermodynamic limit, and $a_n^{(1)}(j;t)$ is a site- and time-dependent perturbation of the form

$$a_n^{(1)}(j;t) = u_{k,n} e^{i(k\cdot j - \omega_k t)} + v_{k,n}^* e^{-i(k\cdot j - \omega_k t)}. \tag{14}$$

Following Refs. [30,32], we linearize the resulting set of equations and find the following eigenvalue problem:

$$\omega_k \begin{pmatrix} \mathbf{u}_k \\ \mathbf{v}_k \end{pmatrix} = \begin{pmatrix} A_k & B_k \\ -B_k & -A_k \end{pmatrix} \begin{pmatrix} \mathbf{u}_k \\ \mathbf{v}_k \end{pmatrix}, \tag{15}$$

where $(\mathbf{u}_k, \mathbf{v}_k)$ are the complex amplitudes of the right- and left-moving waves in the Fock basis, while A_k and B_k are matrices, whose elements take the form

$$\begin{aligned}A_k^{nm} = &-J_0\psi^{(0)}(\sqrt{m}\delta_{m,n+1} + \sqrt{n}\delta_{n,m+1})\\ &+ \left[\frac{U}{2}n(n-1) + \frac{W}{6}n(n-1)(n-2)\right.\\ &\left. + (2J-\mu)n - \hbar\omega_0\right]\delta_{m,n}\\ &- J_k\left[\sqrt{n+1}\sqrt{m+1}a_{n+1}^{(0)}a_{m+1}^{(0)} + \sqrt{n}\sqrt{m}a_{n-1}^{(0)}a_{m-1}^{(0)}\right],\end{aligned} \tag{16}$$

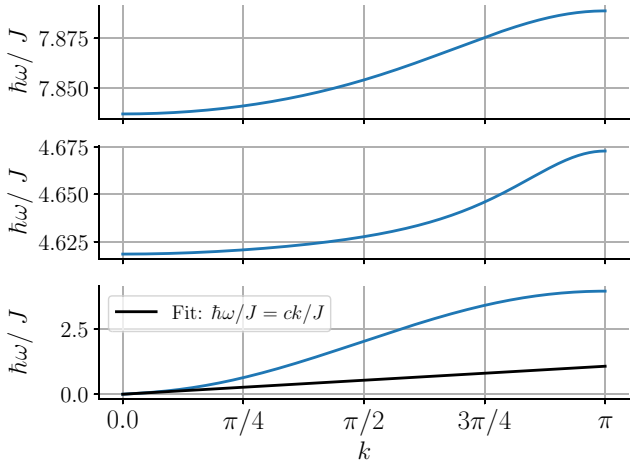

FIG. 3. Low-energy excitations of the liquid. The panels represent (top to bottom) the third, second, and first excitation branches of the system. Moreover, in the lowest panel, we show how, as we should expect, the lowest-energy excitations are phononic (i.e., gapless), and therefore the speed of sound is well defined. The parameters of Hamiltonian Eq. (9) are $U/J = -0.33$, $W/J = 1.39$ and we used $\mu = \mu_0$ as defined in Fig. 2. The parameters of the fit are $c/J = 0.32$. Note that setting $d = 1$ renders k adimensional.

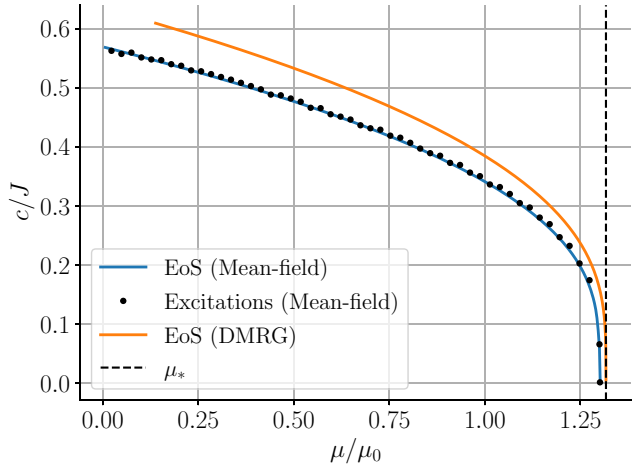

FIG. 4. Speed of sound computed using Eq. (10) with the data from Fig. 2 (blue solid line) and by linearly fitting the lowest branch of the excitation spectrum (see Fig. 3) for small values of the momentum (dots). Each chemical potential is normalized to its equilibrium value ($\mu_0^{\mathrm{DMRG}}/J = -0.040$ and $\mu_0^{\mathrm{MF}}/J = -0.035$) and the vertical line corresponds to the chemical potential of the spinodal point obtained in DMRG $\mu_*^{\mathrm{DMRG}}/J = -0.0057$. The parameters of the Hamiltonian Eq. (9) are $U/J = -0.33$, $W/J = 1.39$.

and

$$B_k^{nm} = -J_k\left[\sqrt{n+1}\sqrt{m}a_{n+1}^{(0)}a_{m-1}^{(0)} + \sqrt{n}\sqrt{m+1}a_{n-1}^{(0)}a_{m+1}^{(0)}\right]. \tag{17}$$

Similarly to $a_n^{(0)}$, the quantity $\psi^{(0)}$ is the lowest-order term of the expansion of Eq. (5) over the homogeneous ground state, that is, it is the order parameter in the thermodynamic limit. Above, we have defined $J_k = 2J(1 - 2\sin(k/2)^2)$, and

$$\hbar\omega_0 = 4J\psi^{(0)2} + \sum_{n=0}\left(\frac{U}{2}n(n-1) + \frac{W}{6}n(n-1)(n-2) + (2J-\mu)n\right)\left|a_n^{(0)}\right|^2. \tag{18}$$

The eigenvalues and eigenvectors of the block matrix in Eq. (15) give the excitation spectrum of the system in the Gutzwiller approximation, see Fig. 3. In particular, from the lowest (nonzero), gapless excitation branch $\omega_k^{(1)}$, we can obtain the speed of sound c, since for $k \to 0$, $\omega_k^{(1)} \to c|k|$ [33], and compare it with that obtained from the equation of state, Eq. (10). In Fig. 4, we plot the speed of sound calculated both using the equation of state and by using a linear fit to the gapless excitation branch for low quasimomenta, at particular values $U/J = -0.33$ and $W/J = 1.39$ of the two- and three-body interaction strengths. There, we observe good agreement between the two approaches.

B. Droplet states

As we have seen, the Gutzwiller approximation supports liquid states at zero temperature. Therefore, besides the homogeneous, thermodynamic ground state, we should expect quantum droplet states with finite particle numbers to exist in the system [8,9,34].

A priori, it is possible to calculate the droplet states by direct local minimization using a dropletlike wave function as a seed. We have followed this procedure and, unfortunately, convergence is very poor as the iterative, numerical procedure tends to either converge towards the vacuum of particles or the homogeneous ground state. We have therefore taken a different route, by minimizing, using an appropriate ansatz, a density functional E_{GW} of the following form:

$$E_{\mathrm{GW}}[\rho] = \sum_j [\rho^{1/2}(j)(\hat{T}\rho^{1/2})(j) + \mathcal{E}_{\mathrm{GW}}(\rho(j))]. \tag{19}$$

Above, $\rho(j)$ is the site-dependent density of the droplet, $\mathcal{E}_{\mathrm{GW}}(\rho)$ is the energy density obtained from the Gutzwiller approximation in the thermodynamic limit, and

$$(\hat{T}f)(j) = -J(f(j+1) + f(j-1) - 2f(j)) \tag{20}$$

is the kinetic-energy term on a lattice. Equation (20) is the discrete analog to the usual lowest-order correction term in density-functional theories of liquids [35,36]. We use the following ansatz [10,37] for the droplet densities,

$$\rho(j\,;\gamma, D) = \frac{N}{dD}\frac{\sinh\left(\frac{\gamma}{2}\right)}{\cosh\left(\frac{\gamma}{2}\right) + \cosh\left(\frac{\gamma}{D}j\right)}. \tag{21}$$

The energy per particle computed by minimizing Eq. (19) with ansatz (21) is presented in Fig. 5. The density above has a central density given by $\rho(0) = \frac{N}{D}\frac{\sinh(\gamma/2)}{1+\cosh(\gamma/2)}$ and exponential tails given by $\rho(j) \sim \exp(-\gamma|j|/2D)$ for large $|j|$. We will later find, see Fig. 6, that these agree with the thermodynamic values $\rho(0) = \rho_0$ and $\gamma/D = \sqrt{-\mu/J}$ [11].

The free parameters in ansatz Eq. (21) are D and γ. Minimizing the functional Eq. (19) with respect to the free parameters, at fixed particle number N, we obtain the energy per particle, central density, and chemical potential as functions of the particle number in vacuum. The energy per particle, in one

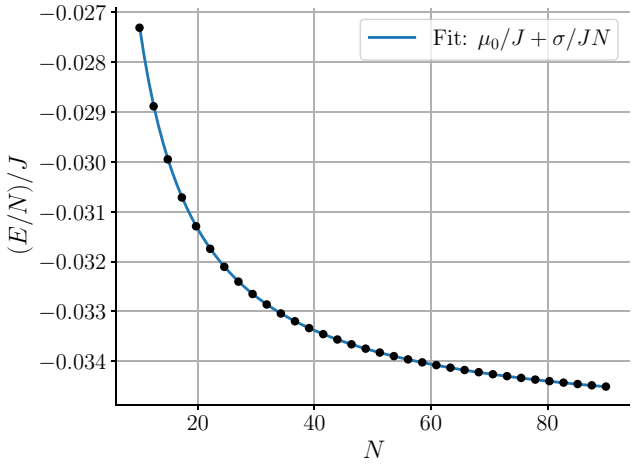

FIG. 5. Energy per particle in terms of the number of particles computed using ansatz Eq. (21). We used the data from Fig. 2 to construct $\mathcal{E}_{\rm GW}$ as shown in Eq. (19). The surface energy obtained from the fit is $\sigma/J = 0.081$. The parameters of the Hamiltonian Eq. (9) are $U/J = -0.33$, $W/J = 1.39$.

dimension, has the following large-N asymptotics [38–40]

$$\frac{E}{N} = \mu_0 + \frac{\sigma}{N} + \frac{g(N)}{N}, \tag{22}$$

where σ is the surface energy of the droplets, and $g(N)$ is a function with $\lim_{N\to\infty} g(N) = 0$ but is nonanalytic in N^{-1}, see Fig. 5. Therefore, the chemical potential behaves, asymptotically, as $\mu = \mu_0 + g(N)$. From the density functional in Eq. (19), and the ansatz in Eq. (21), it can be seen that $g(N)$ may be exponential in the number of particles (see Appendix B).

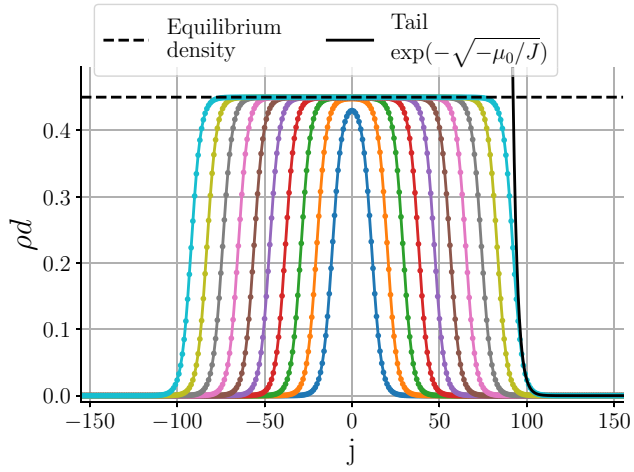

FIG. 6. Droplets profiles computed using ansatz Eq. (21). We used the data from Fig. 2 to construct $\mathcal{E}_{\rm GW}$ as shown in Eq. (19). The parameters of the Hamiltonian Eq. (9) are $U/J = -0.33$, $W/J = 1.39$. From narrowest to broadest, the droplets have, respectively, $N_i = N_0 + i\Delta N$ ($i = 0, 1, \ldots, 9$) particles, with $N_0 = 10$ and $\Delta N = 8.0$.

V. CONCLUSIONS

We have investigated both ground-state properties and low-energy excitations of a Bose-Hubbard model in which, besides the conventional onsite two-body interactions, we have included a contact three-body potential. This extended framework allowed us to study the formation of a self-bound quantum liquid phase building upon previous studies where only gas phases were considered [30]. We made use of the Gutzwiller approximation both in its time-dependent and independent form. We first found that this approach is suitable for studying quantum liquids on a lattice, obtaining an equation of state for a system in which the competition between attractive and repulsive forces gives rise to a self-bound state. We compared our result with those presented in Ref. [11] using DMRG techniques, finding good qualitative agreement between them. A brief discussion is provided on the scope and assumptions under which a direct comparison can be meaningfully made.

As a benchmark for comparing the time-dependent and time-independent approaches, we chose the speed of sound. We computed it in the thermodynamic limit by means of Eq. (10) and compared it with the one obtained from the dispersion relation of gapless excitations in the long-wavelength regime. The agreement found showcases the validity of our analysis.

Moreover, we have studied the formation of droplets in inhomogeneous finite systems. These self-bound states, within the context of ultracold atoms, have been considered primarily incorporating mean-field effects and the inclusion of the Lee-Huang-Yang term [41–43] that takes into account quantum fluctuations. Here we have taken another route and studied droplets that are balanced by the competition of two-body and three-body interactions. The profiles are obtained using a variational approach. Following this procedure, we studied the energetic properties of the droplets and compared them with the predictions of the liquid drop model finding agreement between them. We have discussed the relevance of the nonanalytic (possibly exponential) corrections that are present in the liquid-drop model from a density functional. Since we have limited our study to a variational analysis we have not been able to access the precise functional form of these corrections. A more detailed study of the problem using DMRG or diffusion Monte Carlo (DMC) method of this system, as done in Ref. [11], may attain a much better resolution of the properties of the droplets and provide us with another method to study their dynamical properties.

ACKNOWLEDGMENTS

This work is supported by Grant No. PID2021-126039NA-I00 funded by MICIU/AEI/10.13039/501100011033 and FEDER/EU, grant FPU No. FPU22/03376 funded by MICIU/AEI/10.13039/501100011033 (D.P.-C.), and the Ramón y Cajal Program (Grant No. RYC2020-029961-I) (M.V.), funded by MICIU/AEI/10.13039/501100011033 and by *El FSE invierte en tu futuro*.

DATA AVAILABILITY

The data that support the findings of this article are not publicly available upon publication because it is not

technically feasible and/or the cost of preparing, depositing, and hosting the data would be prohibitive within the terms of this research project. The data are available from the authors upon reasonable request.

APPENDIX A: RANGE OF APPLICABILITY OF THE MEAN-FIELD APPROACH

In this Appendix we study the range of applicability of the mean-field approach to study the Bose-Hubbard model with three-body interactions. In particular, we derive analytical expressions that justify the appearance of a first-order transition to a vacuum state. In the main text we numerically verified that this is the situation with the Gutzwiller approach and in this section we will work out the same result in the context of the one-dimensional Gross-Pitaevskii equation (GPE).

When deriving the GPE for quantum liquids, one defines the solutions by *locally* minimizing the grand-canonical functional. As an example, the functional from which the GPE in Ref. [29] by Astrakharchik and Malomed (AM from now on) is obtained, is given, in their units, by

$$\mathcal{F}_{\rm AM}[\psi,\psi^*] = \int dx\left[-\frac{1}{2}\psi^*\partial_x^2\psi+\frac{1}{2}|\psi|^4-\frac{2}{3}|\psi|^3-\mu|\psi|^2\right]. \quad \text{(A1)}$$

Therefore, the AM equation of state (energy per particle) $e_{\rm AM}(\rho)$ is obtained by setting $\psi=\sqrt{\rho}$, and we have

$$e_{\rm AM}=\tfrac{1}{2}\rho-\tfrac{2}{3}\rho^{1/2}. \quad \text{(A2)}$$

The chemical potential is $\mu=\rho-\rho^{1/2}$ and the physical branch of the density as a function of the chemical potential is simply

$$\rho(\mu)=\left[\frac{1}{2}(1+\sqrt{1+4\mu})\right]^2. \quad \text{(A3)}$$

The equilibrium chemical potential is $\mu_0=-2/9$, and the chemical potential at the spinodal point is $\mu_*=-1/4$. Putting all this together, we see that the locally minimized AM grand potential $\Omega_{\rm AM}$ as a function of length (L) and chemical potential μ, is given by

$$L^{-1}\Omega_{\rm AM}(\mu)=\tfrac{1}{2}[\rho(\mu)]^2-\tfrac{2}{3}[\rho(\mu)]^{3/2}-\mu\rho(\mu). \quad \text{(A4)}$$

For $\mu=\mu_0$, we have $\Omega_{\rm AM}=0$, at which point the vacuuum also minimizes $\Omega_{\rm AM}$. For $\mu_*<\mu<\mu_0$, the absolute minimum occurs for $\psi\equiv 0$, that is, the vacuum. Therefore, if we are willing to describe mean-field liquids at densities that are lower than the equilibrium density, we must accept the local minimum at finite density as valid, for otherwise, the system should be in a state that is empty of particles.

APPENDIX B: ONE-DIMENSIONAL LIQUID-DROP MODEL

Here, we use the lattice version of the liquid-drop model in one spatial dimension and show that, within its framework, the energy per particle in a one-dimensional droplet follows Eq. (22), and that the function $g(N)$ may feature exponential terms.

We begin by assuming that N is large, so that $|\mu/\mu_0-1|\ll 1$, and $|\rho(0)/\rho_0-1|\ll 1$. According to the model, the large majority of particles in the droplet occupy a central plateau with density $\rho(0)\equiv\rho_c$ and diameter D. We then set

$$N=\sum_{j=-D/2}^{D/2}\rho_c \Rightarrow D+1=\frac{N}{\rho_c}. \quad \text{(B1)}$$

We assume that the droplet is leptodermous, so that we may model the surface energy density $\Sigma(j)$ as

$$\Sigma(j)\equiv\frac{\sigma}{2}[\delta_{j,D/2+1}+\delta_{j,-D/2-1}]. \quad \text{(B2)}$$

If we ignore at first kinetic energy contributions, the energy of such a droplet takes the value

$$E=(D+1)\mathcal{E}(\rho_c)+\sigma, \quad \text{(B3)}$$

where $\mathcal{E}(\rho)$ is the energy density in the thermodynamic limit. Using Eq. (B1) to relate particle number and diameter, we obtain

$$\frac{E}{N}=e(\rho_c)+\frac{\sigma}{N}, \quad \text{(B4)}$$

with $e(\rho)$ the energy per particle (equation of state) in the thermodynamic limit. The chemical potential, on the other hand, is independent of the surface energy in one spatial dimension, since

$$\mu(N)=\frac{\partial\mathcal{E}(\rho_c)}{\partial\rho_c}, \quad \text{(B5)}$$

where $\rho_c=\rho_c(N)$. Calling $\delta\rho=\rho_c-\rho_0$, from the liquid drop model without kinetic terms, we would simply have, following Ref. [44], $\partial_N(\delta\rho)=0$, which is special for one spatial dimension. However, this result, within this framework, only means that $\delta\rho(N)$ is not an analytic function of a power of N^{-1}. Nonanalytic deviations, such as exponentials, are not included. Kinetic-energy contributions, negligible in higher dimensions, are exponential. Therefore, we must consider them in one dimension because of the absence of more

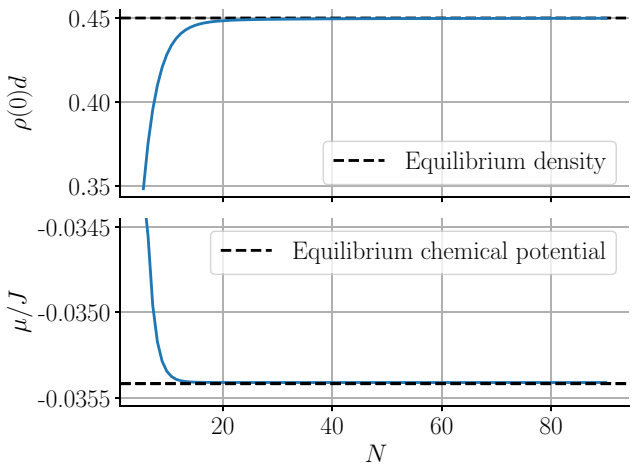

FIG. 7. Central density and chemical potential in terms of the number of particles computed using ansatz Eq. (21). We used the data from Fig. 2 to construct $\mathcal{E}_{\rm GW}$ as shown in Eq. (19). The surface energy obtained from the fit is $\sigma/J=0.081$. The parameters of the Hamiltonian Eq. (9) are $U/J=-0.33$, $W/J=1.39$.

dominant, polynomial contributions. To see this, we may use ansatz Eq. (21) and minimize the grand-canonical functional. The correction of the droplet's chemical potential due to the kinetic energy is given by

$$-J\frac{\partial_x^2\rho^{1/2}}{\rho^{1/2}}\Big|_{x=0} \approx J\left(\frac{\gamma}{D}\right)^2\frac{e^{-\gamma/2}}{2} \approx -\frac{\mu_0}{2}\exp\left(-\frac{\sqrt{-\mu_0/J}}{2\rho_0}N + C\right), \quad \text{(B6)}$$

where C is a constant that accounts for the inaccuracy in setting $D = N/\rho_0$ in the liquid-drop model. This indicates that $g(N)$ in Eq. (22) may be exponential in the number of particles, see Fig. 7. However, the exponent is not necessarily correct, since Eq. (B6) is a local quantity, which is notoriously difficult to reproduce accurately without access to the exact density profile. Moreover, these exponential terms add up to other exponential terms that come from the thermodynamic contribution $\mu = \mu(\rho_c)$. In the particular case of Ref. [29], this is exactly the case, and the kinetic-energy contribution cancels out.

[1] D. Pines and P. Nozières, *The Theory of Quantum Liquids: Normal Fermi liquids*, Advanced Book Classics (CRC Press, Boca Raton, 1989).

[2] C. Cabrera, L. Tanzi, J. Sanz, B. Naylor, P. Thomas, P. Cheiney, and L. Tarruell, Quantum liquid droplets in a mixture of Bose-Einstein condensates, Science **359**, 301 (2018).

[3] M. Schmitt, M. Wenzel, F. Böttcher, I. Ferrier-Barbut, and T. Pfau, Self-bound droplets of a dilute magnetic quantum liquid, Nature (London) **539**, 259 (2016).

[4] I. Ferrier-Barbut, H. Kadau, M. Schmitt, M. Wenzel, and T. Pfau, Observation of quantum droplets in a strongly dipolar Bose gas, Phys. Rev. Lett. **116**, 215301 (2016).

[5] G. Ferioli, G. Semeghini, L. Masi, G. Giusti, G. Modugno, M. Inguscio, A. Gallemí, A. Recati, and M. Fattori, Collisions of self-bound quantum droplets, Phys. Rev. Lett. **122**, 090401 (2019).

[6] F. Böttcher, J.-N. Schmidt, M. Wenzel, J. Hertkorn, M. Guo, T. Langen, and T. Pfau, Transient supersolid properties in an array of dipolar quantum droplets, Phys. Rev. X **9**, 011051 (2019).

[7] G. Semeghini, G. Ferioli, L. Masi, C. Mazzinghi, L. Wolswijk, F. Minardi, M. Modugno, G. Modugno, M. Inguscio, and M. Fattori, Self-bound quantum droplets of atomic mixtures in free space, Phys. Rev. Lett. **120**, 235301 (2018).

[8] D. Petrov, Quantum mechanical stabilization of a collapsing Bose-Bose mixture, Phys. Rev. Lett. **115**, 155302 (2015).

[9] D. Petrov and G. Astrakharchik, Ultradilute low-dimensional liquids, Phys. Rev. Lett. **117**, 100401 (2016).

[10] I. Morera, G. E. Astrakharchik, A. Polls, and B. Juliá-Díaz, Quantum droplets of bosonic mixtures in a one-dimensional optical lattice, Phys. Rev. Res. **2**, 022008 (2020).

[11] I. Morera, B. Juliá-Díaz, and M. Valiente, Universality of quantum liquids and droplets in one dimension, Phys. Rev. Res. **4**, L042024 (2022).

[12] M. Valiente, Three-body repulsive forces among identical bosons in one dimension, Phys. Rev. A **100**, 013614 (2019).

[13] H.-W. Hammer, A. Nogga, and A. Schwenk, *Colloquium*: Three-body forces: From cold atoms to nuclei, Rev. Mod. Phys. **85**, 197 (2013).

[14] T. Sowiński and R. W. Chhajlany, Mean-field approaches to the Bose–Hubbard model with three-body local interaction, Phys. Scr. **2014**, 014038 (2014).

[15] A. Pricoupenko and D. Petrov, Three-body interaction near a narrow two-body zero crossing, Phys. Rev. A **100**, 042707 (2019).

[16] D.-S. Lühmann, Cluster Gutzwiller method for bosonic lattice systems, Phys. Rev. A **87**, 043619 (2013).

[17] I. Carusotto and Y. Castin, An exact reformulation of the Bose–Hubbard model in terms of a stochastic Gutzwiller ansatz, New J. Phys. **5**, 91 (2003).

[18] P. Buonsante, F. Massel, V. Penna, and A. Vezzani, Gutzwiller approach to the Bose-Hubbard model with random local impurities, Phys. Rev. A **79**, 013623 (2009).

[19] M. P. Fisher, P. B. Weichman, G. Grinstein, and D. S. Fisher, Boson localization and the superfluid-insulator transition, Phys. Rev. B **40**, 546 (1989).

[20] D. Jaksch, C. Bruder, J. I. Cirac, C. W. Gardiner, and P. Zoller, Cold bosonic atoms in optical lattices, Phys. Rev. Lett. **81**, 3108 (1998).

[21] M. A. Cazalilla, R. Citro, T. Giamarchi, E. Orignac, and M. Rigol, One dimensional bosons: From condensed matter systems to ultracold gases, Rev. Mod. Phys. **83**, 1405 (2011).

[22] I. Bloch, J. Dalibard, and W. Zwerger, Many-body physics with ultracold gases, Rev. Mod. Phys. **80**, 885 (2008).

[23] D. S. Rokhsar and B. Kotliar, Gutzwiller projection for bosons, Phys. Rev. B **44**, 10328 (1991).

[24] M. C. Gutzwiller, Effect of correlation on the ferromagnetism of transition metals, Phys. Rev. Lett. **10**, 159 (1963).

[25] W. Krauth, M. Caffarel, and J.-P. Bouchaud, Gutzwiller wave function for a model of strongly interacting bosons, Phys. Rev. B **45**, 3137 (1992).

[26] K. Sheshadri, H. Krishnamurthy, R. Pandit, and T. Ramakrishnan, Superfluid and insulating phases in an interacting-boson model: Mean-field theory and the RPA, Europhys. Lett. **22**, 257 (1993).

[27] F. Caleffi, M. Capone, C. Menotti, I. Carusotto, and A. Recati, Quantum fluctuations beyond the Gutzwiller approximation in the Bose-Hubbard model, Phys. Rev. Res. **2**, 033276 (2020).

[28] T. Jolicoeur and J. C. Le Guillou, Fluctuations beyond the Gutzwiller approximation in the slave-boson approach, Phys. Rev. B **44**, 2403 (1991).

[29] G. Astrakharchik and B. A. Malomed, Dynamics of one-dimensional quantum droplets, Phys. Rev. A **98**, 013631 (2018).

[30] K. V. Krutitsky and P. Navez, Excitation dynamics in a lattice Bose gas within the time-dependent Gutzwiller mean-field approach, Phys. Rev. A **84**, 033602 (2011).

[31] J. Zakrzewski, Mean-field dynamics of the superfluid-insulator phase transition in a gas of ultracold atoms, Phys. Rev. A **71**, 043601 (2005).

[32] C. Trefzger, C. Menotti, and M. Lewenstein, Ultracold dipolar gas in an optical lattice: The fate of metastable states, Phys. Rev. A **78**, 043604 (2008).

[33] S. D. Huber, B. Theiler, E. Altman, and G. Blatter, Amplitude mode in the quantum phase model, Phys. Rev. Lett. **100**, 050404 (2008).

[34] Z.-H. Luo, W. Pang, B. Liu, Y.-Y. Li, and B. A. Malomed, A new form of liquid matter: Quantum droplets, Front. Phys. **16**, 32201 (2021).

[35] F. Dalfovo, A. Lastri, L. Pricaupenko, S. Stringari, and J. Treiner, Structural and dynamical properties of superfluid helium: a density-functional approach, Phys. Rev. B **52**, 1193 (1995).

[36] For the droplets, since their average size is much larger than the lattice spacing, we have indistinctly used the usual continuous derivative. Since $J = 1/2m$ the kinetic term reads $T[\rho] = J|\frac{\mathrm{d}\sqrt{\rho}}{\mathrm{d}x}|^2$.

[37] D. Sprung and J. Martorell, The symmetrized Fermi function and its transforms, J. Phys. A: Math. Gen. **30**, 6525 (1997).

[38] S. A. Chin and E. Krotscheck, Structure and collective excitations of ^{4}He clusters, Phys. Rev. B **45**, 852 (1992).

[39] V. Pandharipande, S. C. Pieper, and R. Wiringa, Variational Monte Carlo calculations of ground states of liquid ^{4}He and ^{3}He drops, Phys. Rev. B **34**, 4571 (1986).

[40] S. Stringari and J. Treiner, Systematics of liquid helium clusters, J. Chem. Phys. **87**, 5021 (1987).

[41] T. G. Skov, M. G. Skou, N. B. Jørgensen, and J. J. Arlt, Observation of a Lee-Huang-Yang fluid, Phys. Rev. Lett. **126**, 230404 (2021).

[42] Z. Guo, F. Jia, L. Li, Y. Ma, J. M. Hutson, X. Cui, and D. Wang, Lee-Huang-Yang effects in the ultracold mixture of ^{23}Na and ^{87}Rb with attractive interspecies interactions, Phys. Rev. Res. **3**, 033247 (2021).

[43] T. D. Lee, K. Huang, and C. N. Yang, Eigenvalues and eigenfunctions of a Bose system of hard spheres and its low-temperature properties, Phys. Rev. **106**, 1135 (1957).

[44] J. Treiner, W. Myers, W. Swiatecki, and M. Weiss, Bulk compression due to surface tension in Hartree-Fock, Thomas-Fermi and Droplet-model calculations, Nucl. Phys. A **452**, 93 (1986).